

Off-line and on-line optical monitoring of microalgal growth

Hugo-Enrique Lazcano-Hernandez ¹, Gabriela Aguilar ², Gabriela Dzul ², Rodrigo Patiño ^{Corresp., 2}, Javier Arellano-Verdejo ^{Corresp. 3}

¹ Cátedras CONACYT-El Colegio de la Frontera Sur, Chetumal, Quintana Roo, México

² Departamento de Física Aplicada, Cinvestav Unidad Mérida, Mérida, Yucatán, México

³ Estación para la Recepción de Información Satelital ERIS-Chetumal, El Colegio de la Frontera Sur, Chetumal, Quintana Roo, México

Corresponding Authors: Rodrigo Patiño, Javier Arellano-Verdejo

Email address: rodrigo.patino@cinvestav.mx, javier.arellano@mail.ecosur.mx

The growth of *Chlamydomonas reinhardtii* microalgae cultures was successfully monitored, using classic off-line optical techniques (optical density and fluorescence) and on-line analysis of digital images. In this study, it is shown that the chlorophyll fluorescence ratio F_{685}/F_{740} has a linear correlation with the logarithmic concentration of microalgae. Moreover, with digital images, the biomass concentration was correlated with the luminosity of the images through an exponential equation and the length of penetration of a superluminescent blue beam ($\lambda=440$ nm) through an inversely proportional function. The outcomes of this study are useful to monitor both research and industrial microalgae cultures.

Off-line and on-line optical monitoring of microalgal growth

Hugo E. Lazcano-Hernandez¹, Gabriela Aguilar², Gabriela Dzul², Rodrigo Patiño², and Javier Arellano-Verdejo³

¹Cátedras CONACYT-El Colegio de la Frontera Sur, Chetumal, Quintana Roo, México

²Departamento de Física Aplicada, Cinvestav – Unidad Mérida, Mérida, Yucatán, México

³El Colegio de la Frontera Sur, Estación para la Recepción de Información Satelital ERIS-Chetumal, Chetumal, Quintana Roo, México.

Corresponding author:

Javier Arellano-Verdejo, Rodrigo Patiño

Email address: javier.arellano@mail.ecosur.mx, rodrigo.patino@cinvestav.mx

ABSTRACT

The growth of *Chlamydomonas reinhardtii* microalgae cultures was successfully monitored, using classic off-line optical techniques (optical density and fluorescence) and on-line analysis of digital images. In this study, it is shown that the chlorophyll fluorescence ratio F_{685}/F_{740} has a linear correlation with the logarithmic concentration of microalgae. Moreover, with digital images, the biomass concentration was correlated with the luminosity of the images through an exponential equation and the length of penetration of a super luminescent blue beam ($\lambda=440$ nm) through an inversely proportional function. The outcomes of this study are useful to monitor both research and industrial microalgae cultures.

INTRODUCTION

Photosynthesis is a biophotonic mechanism by which green plants, cyanobacteria and algae transform a fraction of the solar energy to biochemical energy in order to produce their own food. This is the foundation of life on Earth. Photosynthesis occurs in the chloroplasts, which are cell organelles that contain photosynthetic pigments (chlorophyll a, chlorophyll b, carotenoids, etc.). They absorb light and use it to drive photosynthetic light reactions and associated electron transport reactions to reduce CO_2 and oxidize H_2O in the Calvin cycle (Allen, 1992). The net result of photosynthesis is the production of carbohydrates and the release of molecular oxygen to the atmosphere. Environmental factors such as temperature, irradiance, humidity and salinity are known to affect photosynthesis (Rym, 2012).

Currently, microalgae cultivation has been widely studied due to the potential of microalgae as a source of food, biofuel, and various bioactive compounds useful for important processes such as the cleaning of residual waters, CO_2 capture, and H_2 synthesis. All these are valuable products, which contribute to the balance and growth of human activity on a global scale (Gupta et al., 2015). A wide review of on-line and off-line technologies to monitor physicochemical and biological parameters of microalgae was compiled by (Havlik et al., 2016). Although there are several photobioreactors models, in most cases the performance of measurements requires the extraction of samples by syringes or pipettes, which could pollute the culture, disturb algae physiological state, or modify the volume of the medium, to mention only a few disadvantages. Another challenge for real-time measurements is the range increment in the concentration of microalgal cultures, which commonly increases up to three times the original order of magnitude, which is out of the range of most devices (Antal et al., 2019). Therefore, it is currently a challenge to implement non-invasive real-time methodologies for monitoring microalgal cultivation conditions and photosynthetic parameters (Antal et al., 2019).

Chlorophyll (Chl) molecules are organized into two different light systems called Photosystem I (*PSI*) and Photosystem II (*PSII*). Both are spatially separated in the thylakoid membranes of the chloroplasts (Breijo et al., 2006). Every photosystem contains an antenna light-harvesting complex (*LHC*) and central *Chl* molecules. The photosystems differ from each other in their proportions of *Chl a* and *Chl b*, in

46 the characteristics of the reaction centers, and in the electron carriers in their processes. In *PSI*, the
47 reactive center is called *P700* and is formed by two *Chl a* molecules that are attached to each other. *PSII*
48 also contains a reactive center called *P680*, formed also by two *Chl a* molecules. The nomenclature is
49 associated with the maximum wavelength (λ) absorption of both *PSI* and *PSII*: $\lambda=700$ nm and $\lambda=680$ nm,
50 respectively (Gouveia-Neto et al., 2011). According to the origin and kind of *Chl*, the culture medium, the
51 environmental conditions, and the measurement equipment, the maximum fluorescence wavelength may
52 vary. As an example, at room temperature, *Chl a* fluorescence around $\lambda=685$ nm is largely emitted by *PSII*
53 antenna, and fluorescence around $\lambda=740$ nm is emitted by *PSI* antenna (Krause and Weis, 1984; Roháček
54 et al., 2008; Gouveia-Neto et al., 2011). In the fluorescence emission spectra of healthy dilute suspensions
55 of thylakoid membranes or isolated chloroplasts, a sharp peak around $\lambda=685$ nm with a broad shoulder
56 at about $\lambda=740$ nm has been observed (Krause and Weis, 1991). Although isolated *Chl b* dissolved in
57 organic solvent exhibits fluorescence, this does not happen with *in vivo* cultures because the excitation
58 energy is transferred completely to the *Chl a* (Gouveia-Neto et al., 2011).

59 The main function of the *LCH* is to transfer excitation energy to the photosynthetic reaction centers,
60 where photochemical reactions take place; however, a part of the absorbed light energy is dissipated
61 as heat or emitted as fluorescence (Misra et al., 2012). In other words, to return to the ground state,
62 the excited *Chl* molecule undergoes one of three processes: it can be (i) used to drive photochemical
63 reactions (photosynthesis), (ii) dissipated as heat (thermal de-excitation), or (iii) re-emitted as light
64 (fluorescence). These processes occur in competition so that any increase in the efficiency of one will
65 result in a decrease in the yield of the other two. *Chl* fluorescence is an intrinsic signal emitted by plants,
66 algae and cyanobacteria that can be employed to monitor their physiological state, including changes in the
67 photosynthetic apparatus, developmental processes, state of health, stress events, stress tolerance. It can
68 also be used to detect diseases or nutrient deficiency (Gouveia-Neto et al., 2011; Hák et al., 1990). Hence,
69 by measuring the yield of *Chl* fluorescence, information about changes in the efficiency of photosynthesis
70 and heat dissipation can be obtained (Maxwell and Johnson, 2000; Krause and Weis, 1984). Therefore,
71 the simultaneous measuring of *Chl* fluorescence at $\lambda=685$ nm (F_{685}) and at $\lambda=740$ nm (F_{740}) allows for
72 an approximate determination of *Chl* content in a non-destructive way using the *Chl* ratio (F_{685}/F_{740})
73 (Hák et al., 1990).

74 Depending on the type of study and the suitability of the photosynthetic system, different fluores-
75 cence techniques have been used (Mauzerall, 1972; Olson et al., 1996; Kolber et al., 1998; Gorbunov
76 and Falkowski, 2004; Johnson, 2004; Chekalyuk and Hafez, 2008). At present, two *Chl* fluorescence
77 approaches are used to monitor photosynthetic efficiency in microalgae mass cultures: rapid fluorescence
78 induction and the saturation-pulse method (Masojídek et al., 2011), which are well known successful
79 methods. Regarding outdoor algae cultures, specific fluorimeters have been used. The pulse amplitude
80 modulation (*PAM*) fluorimeter provides rapid light responses curves of *PSII*. The dual *PAM* fluorimeter
81 estimates *PSI* and *PSII* yields and the Induction Kinetics fluorimeter measures fluorescence induction
82 curves (Sukenik et al., 2009; Kromkamp et al., 2009; Masojídek et al., 2010). However, real-time non-
83 invasive methodologies are still needed to monitor microalgae culture growth conditions. Therefore, two
84 methodologies are proposed in this study in order to measure *Chlamydomonas reinhardtii* (*C. reinhardtii*)
85 culture growth, through fluorescence measurements at room temperature: an analytic off-line optical
86 technique and an on-line digital images analysis. (*C. reinhardtii*) is considered one of the most promising
87 eukaryotic H_2 producers (Torzillo et al., 2015), which is why its study is relevant. The methodologies
88 proposed here were applied to study the growth of the *C. reinhardtii*. It is possible to apply the proposed
89 methodologies for other species. However, results will vary according to specific strain features, the
90 culture medium, PBR geometry, light sources and temperature. However, the methodologies are simple
91 and easy to install and assess.

92 1 MATERIALS AND METHODS

93 This project aimed at identifying alternative optical techniques for monitoring microalgal growth. Our hy-
94 potheses were that *C. reinhardtii* culture cell concentration correlates with (1) the off-line *Chl* fluorescence
95 ratio F_{685}/F_{740} , (2) the on-line images culture color, and (3) the on-line image culture fluorescence.

96 1.1 Microalgae cultures

97 The *C. reinhardtii* (CC-124) microalgae were purchased from the Chlamydomonas Resource Center
98 (USA) and grown photoautotrophically in Sueoka medium (Sueoka, 1960). Growth conditions include

continuous air bubbling ($1VVM = 1L - air/min/L - medium$) under controlled room temperature conditions (298 ± 2) K. Experiments were performed in two series: firstly for the off-line optical density and fluorimetry measurements (Experiments A and B), and then for the on-line techniques using digital images (Experiments 1 to 5). A portable spectrometer (*StellarNet, EPP2000*) was used to measure optical density, fluorescence and color of the microalgae cultures, with a detection range between 200 and 850 nm. The corresponding Spectrawiz software (*StellarNet, OS V5.0* ©2011) was used for spectrometer measurements. In order to follow the cell growth, optical density (OD) measurements at $\lambda = 640$ nm were taken; each measurement was repeated three times for every sample. In a previous study, the dry weight of the microalgae has been correlated with the OD of the algae cultures (del Campo et al., 2014). Limitations of the OD technique as well as its applications to other species and another culture medium were discussed by (Griffiths et al., 2011).

For the off-line experiments, three 1-L Roux culture bottles were used, each with 0.9L of algae culture, with continuous air bubbling ($1L/min$), under controlled room temperature conditions (figure 1a). The cultures were illuminated continuously with two fluorescent lamps (Philips, *F20T12/D20W*). To assess the microalgae growth kinetics, three samples of 3mL each were taken from every bottle every 12 hours for five days; additionally, a final control measurement was taken on the seventh day. Triplicate OD and fluorescence measurements were taken for every sample. Two experiments were performed with the only difference for the initial microalgae concentration, x_0 : Experiment A, $x_0 = (34 \pm 2)mg/L$, and Experiment B, $x_0 = (42 \pm 2)mg/L$. In summary, a total of 270 measurements were made for every of-line experiments. Therefore, the number of measurements provides statistical significance to this study.

For the on-line experiments, a 3-L column photo-bio-reactor (*PBR*) was used. A transparent acrylic tube with a thickness of 25 mm and an inner diameter of 95 mm was used to build the 95-cm length *PBR*. Four fluorescent lamps (Tecno Lite, *T46500K20W*) were used to illuminate the center of the column with around $100 \mu mol$ photons $m^{-2}s^{-1}$. To avoid external light, the *PBR* was placed inside a dark cabin (figure 1b). Five experiments were performed, each during five days: three experiments with continuous illumination (Experiments 1, 2, and 3), and two experiments with 12-h light/12-h dark cycles (Experiments 4 and 5). Both off-line samples and digital images were taken every 6 or 12 h. A webcam (*Logitech, Carl Zeiss Tessar HD 1080 p*) connected to a PC was used to capture *PBR* digital images. For the color analysis, the images were captured with two fluorescent lamps turned on behind the *PBR* while the other two lamps remained turned off. For the fluorescent images, the pictures were captured in darkness and only illuminated with a blue beam from a super luminescent diode (maximal wavelength of 440 nm) and a light filter (*LSR-GARD ARGON, model 2204*) with a protection range in 190-520 nm. In order to measure fluorescence after a dark-adapted period, at least 15 min of darkness were provided before fluorescent stimulation. The images were analyzed in a LCD screen with an Integrating cube (*StellarNet, IC2*) and the portable spectrometer. The International Commission on Illumination (CIE LAB) scale was used for color measurements. To achieve a homogeneous representation of the color of every image, five measurements were taken from different regions of the *PBR*.

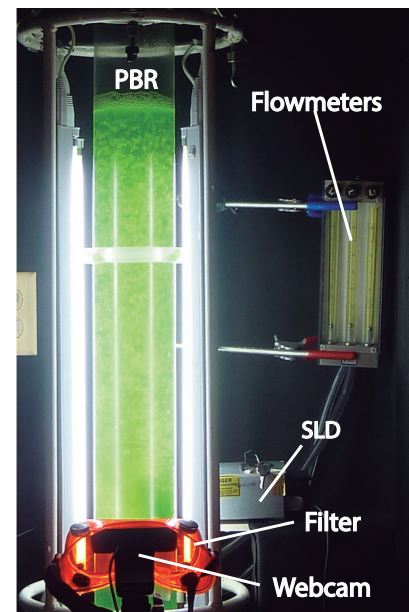
1.2 Fluorescence cabin

The experimental system to measure fluorescence was composed of two main parts: a fluorescence cabin and the portable spectrometer. Based on the spectrometer, the fluorescence cabin was designed, manufactured, and coupled to the system using an optical fiber (*StellarNet, F400*). Through this fiber, light was guided from the sample cuvette to the spectrometer detector. The fluorescence cabin configuration is shown in Figure 2a. The main components are a dark cabin, a cylindrical (14 mm i.d.) glass sample cuvette (4 mL), light emission diodes (LED), feed and switching electronic circuits, an AC/DC electric current converter (output 5.4 V), and a multi-modal optical fiber connector. The dark cabin is a space where light does not come in from external sources. Inside the dark cabin, a base was used to fix the cuvette in a normal position (at 90 degrees) relative to the floor. Parallel to the floor, as exciting radiation, six LEDs were placed (Stereon, Ultra Blue), three to the right side of the sample cuvette and three to the left. This configuration ensured homogeneous illumination conditions. In Figure 2b, the spectrum of the six LEDs is shown, with a maximum wavelength emission around $\lambda=464$ nm, luminosity of 7 cd and 400 mW as maximum power.

To improve fluorescence measurements quality, the optical fiber was positioned on the top of the glass sample cuvette, at 90° relative to the LEDs radiation. Traditionally, fluorescence is measured through the sample cuvette wall. Instead of that, fluorescence measurements were taken on the uncovered top of the



(a)



(b)

Figure 1. (a) The three Roux bottles for the off-line experiments (A and B), and (b) the column photo-bio-reactor (PBR) for the on-line experiments (1-5), Super Luminescent Diode (SLD); see Materials and Methods

153 cuvette, thus achieving diminishing losses by reflection and refraction in the interface of the cuvette. The
 154 cuvette used for the samples was a 4-mL glass cylinder, but with this fluorescence system, the material
 155 and the geometry of the cuvette are not important. The light information was processed and digitalized
 156 by the spectrometer SpectraWiz software. Before measurements, the reference blank was defined by
 157 setting the spectrometer with Sueoka medium; then, the fluorescence measurement was performed on
 158 the microalgae sample. The direct fluorescence of *C. reinhardtii* culture samples at room temperature
 159 was measured successfully throughout seven days with this experimental setup. The ratio of fluorescence
 160 intensity between $\lambda=685$ and $\lambda=740$ nm was calculated.

161 1.3 The F_{685}/F_{740} fluorescence ratio

162 At low *Chl* concentrations, fluorescence emissions increase with increasing amounts of *Chl*. At higher
 163 concentrations, the increase of fluorescence with the increment of *Chl* is mainly detected around 740 nm.
 164 For in vivo cultures, fluorescence emission at 740 nm is favored (and fluorescence emission at 685 nm is
 165 not favored), because of (i) the re-absorption of photons from the fluorescence emitted by neighboring
 166 molecules, (ii) the light interference between the short (685 nm) and long wavelengths (740 nm), and
 167 (iii) the increment of *Chl* (the new *Chl* molecules preferentially absorb energy at 685 nm) (Gouveia-Neto
 168 et al., 2011).

169 There is a good inverse correlation between photochemistry and *Chl* fluorescence. The ratio of
 170 fluorescence intensity between maximal wavelengths (F_{685}/F_{740}) is influenced by photosynthetic activity.
 171 In mature microalgae cultures, the chloroplast structure, CO_2 uptake rate, carbon metabolism, etc.,
 172 are better than in the younger cells. Higher F_{685}/F_{740} values signal young cultures or cultures with
 173 photosynthetic apparatus not yet fully developed. Low values of this rate indicate mature cultures with a
 174 fully developed photosynthetic apparatus. In other words, the decrement in F_{685}/F_{740} value is indicative
 175 of increased photosynthetic activity. Measured through induction fluorescence, F_{685}/F_{740} exhibits a
 176 curvilinear relationship with cells concentration (x), which can be successfully expressed by equation 1,
 177 where c and d are constants (Hák et al., 1990):

$$\frac{F_{685}}{F_{740}} = cx^{-d} \quad (1)$$

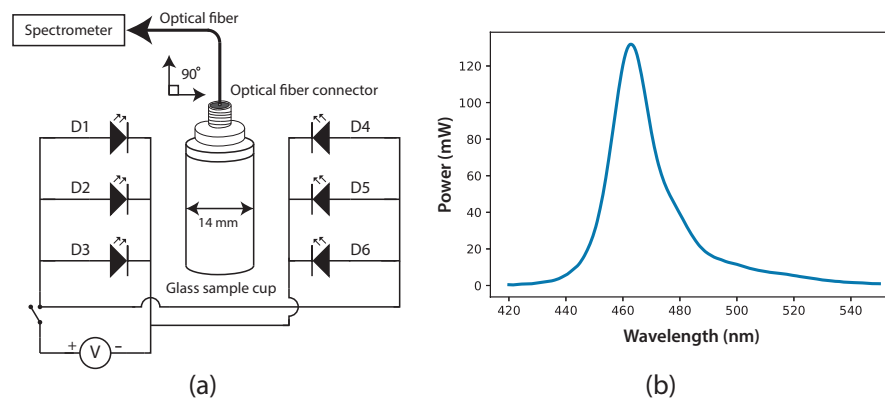


Figure 2. (a) Fluorescence cabin diagram, with optical fiber connector and glass sample cuvette; six Ultra Blue LEDs were installed as exciting source. (b) Spectrum of the exciting radiation source (Ultra Blue LEDs, $\lambda_{\text{max}} = 464 \text{ nm}$)

178 This technique has been applicable to all kinds of leaves, chloroplast suspensions and acetone extracts
 179 of photosynthetic pigments. In this study, it was demonstrated that this technique is also applicable to
 180 microalgae cultures.

181 2 RESULTS AND DISCUSSION

182 2.1 Microbial growth

183 It has been established in a previous work that the Gompertz model represents the *C. reinhardtii* growth
 184 better than the classical Monod model (del Campo et al., 2014). Actually, the Monod and Gompertz
 185 models can be seen as particular cases of a more universal growth model (Castorina et al., 2006). For the
 186 experiments in the Roux bottles (A and B), as well as in the *PBR* (1-5), the Gompertz specific growth
 187 rate is reported in table 1. For the *PBR* experiments, it was possible to observe that Gompertz model is
 188 best fitted when the light regime is continuous (see R^2 for experiments 1-3) than when light/dark cycles
 189 are performed (experiments 4-5). Moreover, the specific growth rate is favored when the *PBR* is used, in
 190 contrast with the cultures in the Roux bottles.

Reactor	Experiments	$\mu(\text{day}^{-1})$	R^2
Roux bottles	AI	0.5472	0.9981
	AII	0.5856	0.9989
	AIII	0.5424	0.9889
		0.56 ± 0.02	
	BI	0.3360	0.9843
	BII	0.4032	0.9965
PBR	3	0.3696	0.9944
		0.37 ± 0.03	
	1	0.7824	0.9954
	2	0.6720	0.9771
	3	0.6192	0.9656
	0.69 ± 0.08		
	4	0.3384	0.9180
	5	0.4776	0.9312
		0.41 ± 0.10	

Table 1. The Gompertz specific growth rate of microalgae in seven experiments, with the corresponding correlation values. The mean value and the standard deviation are reported for the cultures with continuous illumination (experiments A and B in the Roux bottles, and 1, 2, and 3 in the *PBR*) and with light/dark cycles (experiments 4 and 5 in the *PBR*).

2.2 Fluorescence measurements

The variations in fluorescence intensity were successfully measured according to the increment in *C. reinhardtii* concentration. Some selected spectra are shown in Figure 3 for experiment A. The fluorescence dataset for experiments A and B are shown in supplementary material file (S1). In all cases, *Chl* fluorescence exhibits a peak around $\lambda=685$ nm and a broad shoulder around $\lambda=740$ nm; this is a general observation at room temperature for *Chl a* (Gouveia-Neto et al., 2011; Krause and Weis, 1984). The fluorescence around $\lambda=685$ nm is attributed to the *PSII* antenna, and the fluorescence around $\lambda=740$ nm is due to the *PSI* antenna (Gouveia-Neto et al., 2011). The fluorescence signal/noise ratio in measurements was around 7 at $\lambda=740$ nm and 14 at $\lambda=685$ nm.

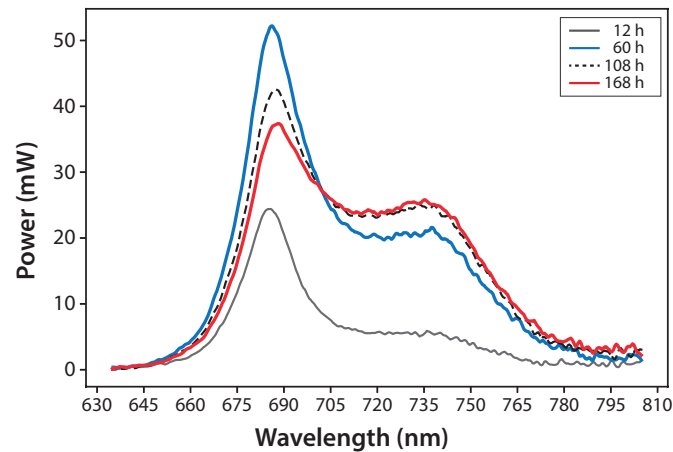


Figure 3. Microalgae fluorescence emission spectra ($298 \pm 2K$): evolution throughout seven days (168 h). Experiment A, $x_0 = (34 \pm 2)$ mg/L

In Figure 4, fluorescence evolution at $\lambda=685$ nm and at $\lambda=740$ nm is shown for all bottles of experiments A. The plots include trend lines. In both experiments A and B, the maximum fluorescence intensity at $\lambda=685$ nm occurred between 48 and 60 hours. After that time fluorescence decreased. Regarding fluorescence at $\lambda=740$ nm, in Experiment A, the maximum value occurred at 72 hours in all cultures; and in Experiment B, the maximum value happened between 96 and 108 hours. For both experiments, the maximum fluorescence at $\lambda=685$ nm occurred before than at $\lambda=740$ nm. And maximum fluorescence at $\lambda=740$ nm occurred at the highest concentrations of algae. In general, the results are consistent with those described in the literature for fluorescence in plants (Gouveia-Neto et al., 2011). Namely, at low *Chl* concentrations, fluorescence emissions increase with increasing *Chl* concentration. At higher concentrations, the increase of fluorescence with the increment of *Chl* was detected only around $\lambda=740$ nm.

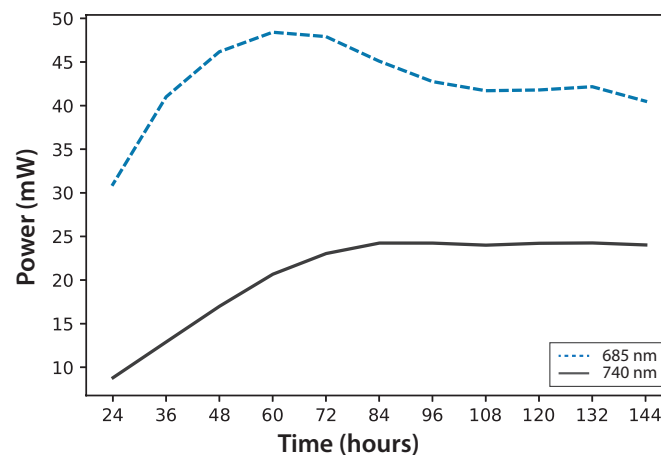


Figure 4. Experiment A: *C. reinhardtii* Fluorescence evolution trend at $\lambda = 685$ nm and $\lambda = 740$ nm

210 Regarding the F_{685}/F_{740} ratio, it was possible to observe a similar behavior in every culture of both
 211 experiments, regardless of the initial concentration. For that reason, Figure 5 shows the average of the
 212 three cultures for each of the two experiments over five days, and a final measurement on the seventh
 213 day. As time went by, the F_{685}/F_{740} fluorescence ratio decreased, and that means that the photosynthetic
 214 processes were improved. The same trend has been reported for green leaves in plants, as stated in
 215 equation 1 (Hák et al., 1990).

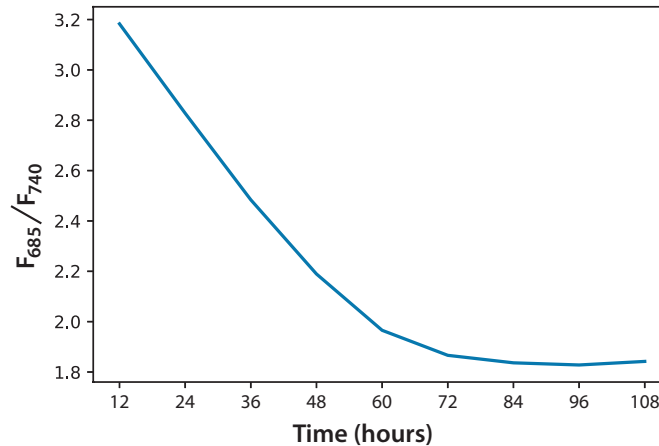


Figure 5. Fluorescence ratio (F_{685}/F_{740}) trend for *C. reinhardtii*

216 Based on the information in Figure 5, and considering the data of 168 hours as the minimum possible
 217 (aged cultures), we figured that cultures in both experiments reached around 70% of maturity at 96 hours.
 218 Therefore, every culture evolved successfully, which means that the conditions are appropriate to grow
 219 the microalgae and keep them in a good state of health. In addition, the cultures that reached the lowest
 220 F_{685}/F_{740} values, that is, the highest photosynthetic activity, were those of Experiment A, which started
 221 with the lowest initial concentration. Moreover, after 72 hours, these values did not change significantly.
 222 This is the moment when illumination may not be enough for the culture because cell concentration
 223 reduces the passage of light. Finally, equation 2 expressed a very useful linear correlation between the
 224 logarithmic concentration of microalgae and the F_{685}/F_{740} ratio through time (Figure 6):

$$\ln\left(\frac{x}{x_0}\right) = 3.27 - 0.7084(F_{685}/F_{740}) \quad (2)$$

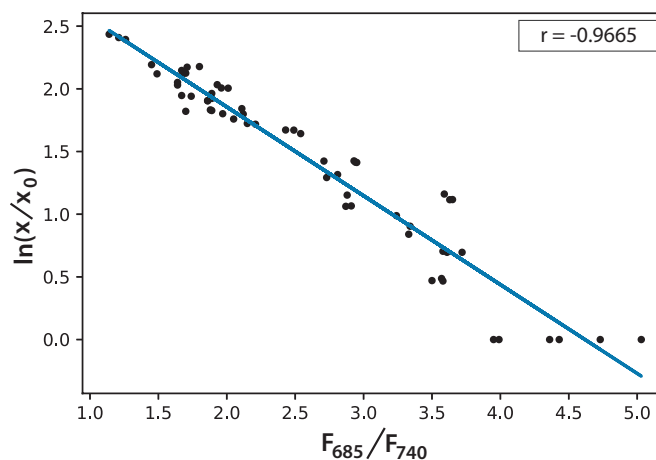


Figure 6. Linear correlation for the logarithmic microalgae concentration and the fluorescence ratio F_{685}/F_{740} ($r = -0.966578$)

2.3 Digital images

When the *PBR* was used, digital images of the cultures were taken to follow the change in color and to measure the penetration of a fluorescent beam during the microalgae growth. A selection of images is presented in Figure 7 for a typical experiment. It was possible to observe that cultures get darker with time due to the increase of biomass concentration in the *PBR*, which prevents the passage of light throughout the reactor. For the fluorescence measurements, the flashes due to the blue super-luminescent diode were filtered in order to measure only the fluorescence light contribution, which diminishes with time due to a shadow effect by cells when the microalgae concentration gets denser.

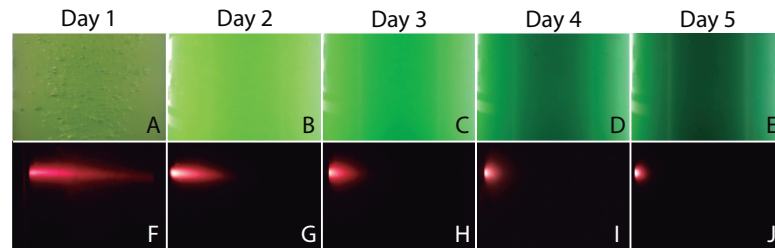


Figure 7. Representative images of the *PBR* captured every day during an experiment. Color assessment (Figures 7A-7E) and Fluorescent beam penetration (Figures 7F-7J).

CIELAB measurements include three values to characterize the color of a sample: *L* is the luminosity, the parameter “*a*” for colors from green to red, and the parameter “*b*” for colors from blue to yellow. Both “*a*” and “*b*” parameters remained almost constant throughout the experiment during microalgae growth. This means that, technically, color does not change, which is expected since the photosynthetic pigments are always the same. In fact, luminosity is what diminishes importantly during cell growth since cells deviate or shadow light sources. In Figure 8, it is possible to observe the logarithmic correlation between the microalgae concentration *x*, and the luminosity *L* for experiments 1-3. For these experiments, equation 3 is proposed to get *x* from on-line measurements of *L* from digital images:

$$\ln\left(\frac{x}{x_0}\right) = (1.6 \pm 0.2) - (0.44 \pm 0.04)(L/W) \quad (3)$$

In this equation, the intercept and the slope values are presented as the mean and the corresponding standard deviation of the individual correlations in the three experiments (see Figure 8). However, this same correlation was not observed in experiments 4-5, where light/dark cycles were performed (Figure 9). A calculation of the correlations between the values of the three experiments confirms that the experiments are reproducible, which gives confidence to the study. Table 2 shows the *L(W)* and Table 3 shows the correlation between $\ln(x/x_0)$ values.

	E1	E2	E3
E1	1.000000	0.963332	0.942350
E2	0.963332	1.000000	0.973427
E3	0.942350	0.973427	1.000000

Table 2. *L(W)* Correlation

	E1	E2	E3
E1	1.000000	0.973283	0.948333
E2	0.973283	1.000000	0.985426
E3	0.948333	0.985426	1.000000

Table 3. $\ln(x/x_0)$ Correlation

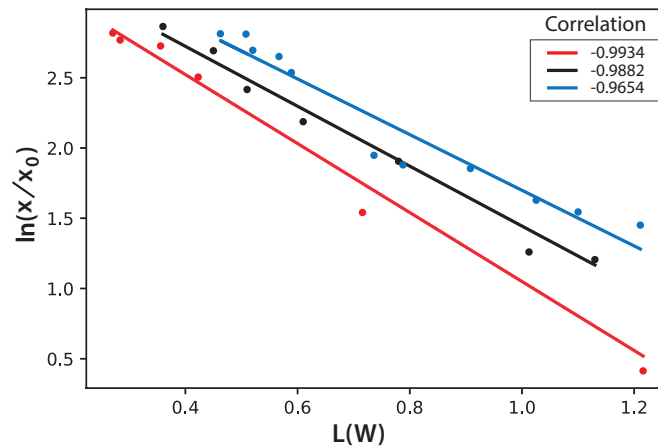


Figure 8. Logarithmic dependence of cell concentration with the luminosity (L) value in the CIELAB scale of colors, for the PBR experiments with continuous illumination. The colors correspond to experimental values: black (exp. 1), red (exp. 2), and blue (exp. 3); the lines correspond to the mean-squares correlations

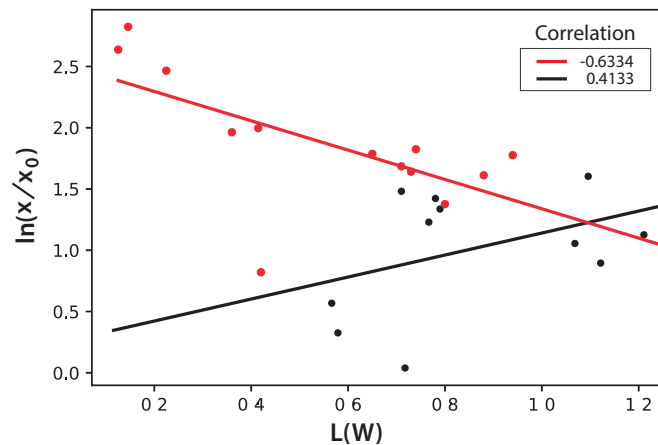


Figure 9. Logarithmic dependence of cell concentration with the luminosity (L) value in the CIELAB scale of colors, for the PBR experiments with light/dark cycles. The colors correspond to experimental values: black (exp. 4), red (exp. 5); the lines correspond to the mean-squares correlations

247 Finally, the fluorescence beam penetration was characterized as an image changing with time. Both the
 248 beam surface area (data not shown) and penetration distance were used to follow these changes. Similar
 249 results were obtained when comparing the cell concentration with the changes in the fluorescent images;
 250 therefore, only the distance beam penetration was used since its measurement is much simpler than that
 251 of the surface area. In Figure 10, it is possible to observe the correlation of this distance measured for the
 252 fluorescent beam penetration with the inverse of the OD. As stated before, the OD is already related with
 253 the biomass concentration (del Campo et al., 2014). It is important to notice that the linear correlations
 254 were obtained for all 1-5 experiments, with equation 4 proposed to calculate the OD of the culture directly
 255 from the on-line measure of the beam penetration:

$$OD = \frac{1}{\text{beam penetration / cm}} \quad (4)$$

256 This simple equation is proposed since the values for the mean and the corresponding standard
 257 deviation for the intercept and the slope in the individual linear correlations for the five experiments are,
 258 respectively, (0.0 ± 0.5) and $(1.0 \pm 0.1) \text{ cm}^{-1}$.

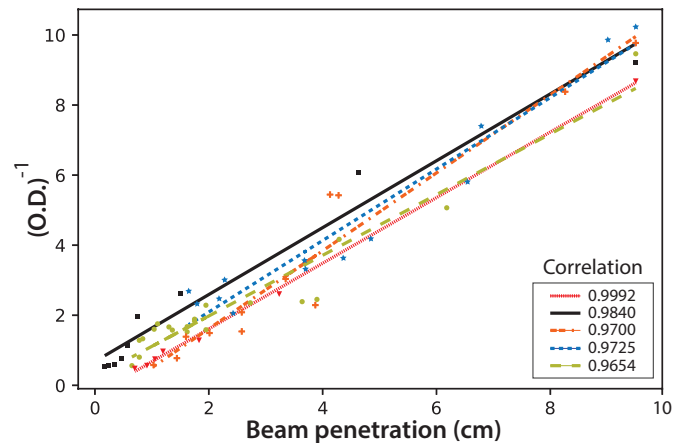


Figure 10. The inverse of the optical density (OD) for the microalgae cultures, as a function of the fluorescent beam penetration in the PBR. The colors correspond to the experimental values: red dash line (exp. 1), black (exp. 2), orange dotted line (exp. 3), blue dotted line (exp. 4) and light green dotted line (exp. 5); the lines correspond to the least-squares correlations.

3 CONCLUSIONS

The growth of *C. reinhardtii* cultures was successfully monitored through off-line and on-line optical techniques at an affordable cost. It was confirmed that, as evidenced in green plants, the maximum fluorescence around $\lambda=685$ nm occurs before than that happening at $\lambda=740$ nm. The maximum fluorescence at $\lambda=740$ nm occurs at a higher concentration, compared to what is needed at $\lambda=685$ nm. Once the maximum fluorescence at $\lambda=685$ nm has been reached, its decrement occurs before and at a faster rate that the fluorescence at $\lambda=740$ nm. Although the F_{685}/F_{740} fluorescence ratio is a method that has been well known, here it was demonstrated for *C. reinhardtii* cultures. A very useful linear correlation occurs between logarithmic concentration of *C. reinhardtii* and the F_{685}/F_{740} ratio through time.

Moreover, the on-line analysis of digital images was shown to be also useful to track *C. reinhardtii* growth. The luminosity measurements in the CIELAB scale were linearly correlated with the microbial concentration for cultures under continuous illuminations; however, for the cultures in a light/dark regime, this correlation was not found. Nevertheless, for the fluorescent beam penetration images, both the distance and the surface captured for the beam were linearly correlated with the optical density and, consequently, with the microalgae culture density for all the illumination regimes. Indeed, a simple reciprocal equation can be used to calculate the optical density as the inverse of the measured distance of the beam penetration.

The on-line techniques proposed here are very practical to study both research and industrial microalgae cultures. As a future study, in the case of having multispectral remote sensing reflectances both at 685 nm and 740 nm, and with the contribution of field measurements for calibration, it would be feasible to use equation 2 and regression models between the logarithmic concentration of microalgae and remote sensing data to estimate the concentration of Chlorophyll a in water wide areas.

ACKNOWLEDGMENTS

Hugo Lazcano thanks CONACyT for his postdoctoral fellowship and for the support provided through the "Cátedras-CONACYT" program (project 526). The authors are grateful to the reviewers for their contribution to improve this manuscript. We thank Moisés Perales for his help with editing the manuscript.

FUNDING

This research did not receive any specific grant from funding agencies in the public, commercial, or not-for-profit sectors.

288 **REFERENCES**

- 289 Allen, J. F. (1992). How does protein phosphorylation regulate photosynthesis? *Trends in biochemical*
290 *sciences*, 17(1):12–17.
- 291 Antal, T., Konyukhov, I., Volgusheva, A., Plyusnina, T., Khruschev, S., Kukarskikh, G., Goryachev, S.,
292 and Rubin, A. (2019). Chlorophyll fluorescence induction and relaxation system for the continuous
293 monitoring of photosynthetic capacity in photobioreactors. *Physiologia plantarum*, 165(3):476–486.
- 294 Breijo, F. J. G., Caselles, J. R., and Siurana, P. S. (2006). *Introducción al funcionamiento de las plantas*.
295 Ed. Univ. Politéc. Valencia.
- 296 Castorina, P., Delsanto, P., and Guiot, C. (2006). Classification scheme for phenomenological universalities
297 in growth problems in physics and other sciences. *Physical review letters*, 96(18):188701.
- 298 Chekalyuk, A. and Hafez, M. (2008). Advanced laser fluorometry of natural aquatic environments.
299 *Limnology and Oceanography: Methods*, 6(11):591–609.
- 300 del Campo, J. S. M., Escalante, R., Robledo, D., and Patino, R. (2014). Hydrogen production by
301 *Chlamydomonas reinhardtii* under light-driven and sulfur-deprived conditions: using biomass grown
302 in outdoor photobioreactors at the Yucatan peninsula. *International journal of hydrogen energy*,
303 39(36):20950–20957.
- 304 Gorbunov, M. Y. and Falkowski, P. G. (2004). Fluorescence induction and relaxation (fire) technique and
305 instrumentation for monitoring photosynthetic processes and primary production in aquatic ecosystems.
306 In *Photosynthesis: Fundamental Aspects to Global Perspectives*—Proc. 13th International Congress of
307 *Photosynthesis, Montreal, Aug*, pages 1029–1031.
- 308 Gouveia-Neto, A. S., da Silva-Jr, E. A., Cunha, P. C., Oliveira-Filho, R. A., Silva, L. M., da Costa, E. B.,
309 Camara, T. J., and Willadino, L. G. (2011). Abiotic stress diagnosis via laser induced chlorophyll
310 fluorescence analysis in plants for biofuel. In *Biofuel Production—Recent Developments and Prospects*.
311 IntechOpen.
- 312 Griffiths, M. J., Garcin, C., van Hille, R. P., and Harrison, S. T. (2011). Interference by pigment in the
313 estimation of microalgal biomass concentration by optical density. *Journal of microbiological methods*,
314 85(2):119–123.
- 315 Gupta, P. L., Lee, S.-M., and Choi, H.-J. (2015). A mini review: photobioreactors for large scale algal
316 cultivation. *World Journal of Microbiology and Biotechnology*, 31(9):1409–1417.
- 317 Hák, R., Lichtenthaler, H., and Rinderle, U. (1990). Decrease of the chlorophyll fluorescence ratio
318 f_{690}/f_{730} during greening and development of leaves. *Radiation and environmental biophysics*,
319 29(4):329–336.
- 320 Havlik, I., Scheper, T., and Reardon, K. F. (2016). *Monitoring of Microalgal Processes*, pages 89–142.
321 Springer International Publishing, Cham.
- 322 Johnson, Z. I. (2004). Description and application of the background irradiance gradient-single turnover
323 fluorometer (big-stf). *Marine Ecology Progress Series*, 283:73–80.
- 324 Kolber, Z. S., Prášil, O., and Falkowski, P. G. (1998). Measurements of variable chlorophyll fluorescence
325 using fast repetition rate techniques: defining methodology and experimental protocols. *Biochimica et*
326 *Biophysica Acta (BBA)-Bioenergetics*, 1367(1-3):88–106.
- 327 Krause, G. and Weis, E. (1991). Chlorophyll fluorescence and photosynthesis: the basics. *Annual review*
328 *of plant biology*, 42(1):313–349.
- 329 Krause, G. H. and Weis, E. (1984). Chlorophyll fluorescence as a tool in plant physiology. *Photosynthesis*
330 *research*, 5(2):139–157.
- 331 Kromkamp, J. C., Beardall, J., Sukenik, A., Kopecký, J., Masojádek, J., Van Bergeijk, S., Gabai, S.,
332 Shaham, E., and Yamshon, A. (2009). Short-term variations in photosynthetic parameters of nan-
333 nochloropsis cultures grown in two types of outdoor mass cultivation systems. *Aquatic Microbial*
334 *Ecology*, 56(2-3):309–322.
- 335 Masojádek, J., Kopecký, J., Giannelli, L., and Torzillo, G. (2011). Productivity correlated to photobio-
336 chemical performance of *Chlorella* mass cultures grown outdoors in thin-layer cascades. *Journal of*
337 *industrial microbiology & biotechnology*, 38(2):307–317.
- 338 Masojádek, J., Vonshak, A., and Torzillo, G. (2010). Chlorophyll fluorescence applications in microalgal
339 mass cultures. In *Chlorophyll a fluorescence in aquatic sciences: methods and applications*, pages
340 277–292. Springer.
- 341 Mauzerall, D. (1972). Light-induced fluorescence changes in *Chlorella*, and the primary photoreactions
342 for the production of oxygen. *Proceedings of the National Academy of Sciences*, 69(6):1358–1362.

- 343 Maxwell, K. and Johnson, G. N. (2000). Chlorophyll fluorescence—a practical guide. *Journal of*
344 *experimental botany*, 51(345):659–668.
- 345 Misra, A. N., Misra, M., and Singh, R. (2012). Chlorophyll fluorescence in plant biology. In *Biophysics*.
346 IntechOpen.
- 347 Olson, R. J., Chekalyuk, A. M., and Sosik, H. M. (1996). Phytoplankton photosynthetic characteristics
348 from fluorescence induction assays of individual cells. *Limnology and oceanography*, 41(6):1253–1263.
- 349 Roháček, K., Soukupová, J., and Barták, M. (2008). Chlorophyll fluorescence: a wonderful tool to study
350 plant physiology and plant stress. *Plant Cell Compartments-Selected Topics. Research Signpost, Kerala,*
351 *India*, pages 41–104.
- 352 Rym, B. D. (2012). Photosynthetic behavior of microalgae in response to environmental factors. In
353 *Applied Photosynthesis*. IntechOpen.
- 354 Sueoka, N. (1960). Mitotic replication of deoxyribonucleic acid in *chlamydomonas reinhardi*. *Proceedings*
355 *of the National Academy of Sciences of the United States of America*, 46(1):83.
- 356 Sukenik, A., Beardall, J., Kromkamp, J. C., Kopecký, J., Masojídek, J., van Bergeijk, S., Gabai, S.,
357 Shaham, E., and Yamshon, A. (2009). Photosynthetic performance of outdoor nanochloropsis mass
358 cultures under a wide range of environmental conditions. *Aquatic Microbial Ecology*, 56(2-3):297–308.
- 359 Torzillo, G., Scoma, A., Faraloni, C., and Giannelli, L. (2015). Advances in the biotechnology of
360 hydrogen production with the microalga *chlamydomonas reinhardtii*. *Critical reviews in biotechnology*,
361 35(4):485–496.